Multilevel hierarchical topographies by combined photolithography and nanoimprinting processes to create surfaces with controlled wetting

María T. Alameda, Manuel R. Osorio, Jaime J. Hernández* and Isabel Rodríguez

Multilevel Hierarchical Topographies by Combined Photolithography and Nanoimprinting Processes to Create Surfaces with Controlled Wetting

María T. Alameda, Manuel R. Osorio, Jaime J. Hernández and Isabel Rodríguez*

Madrid Institute for Advanced Studies in Nanoscience (IMDEA Nanoscience),

C/Faraday 9, Ciudad Universitaria de Cantoblanco, Madrid 28049, Spain.

KEYWORDS

Nanoimprinting lithography, anisotropic wetting, nanofabrication, hierarchical structure, fractal, bioinspired

ABSTRACT

This work presents a practical methodology to produce multilevel hierarchical structures with precise control of the structural geometry at every level by combining photo and nanoimprint lithography processes. The method involves sequential steps of nanoimprinting of a first deposited polymer layer followed by nanoimprinting of a second deposited layer of a photo-resin and afterwards, performing on this layer optical lithography by means of a maskless laser writer to pattern micron-size features. A

hierarchical topography is consequently obtained comprising nanopatterns and micropatterns at different levels designed independently with very high feature control. The process can be repeated sequentially employing hierarchical working molds produced on a previous fabrication cycle to produce multilevel self-similar hierarchical topographies in a sort of fractal growing manner. The patterning method has broad applicability, as exemplary demonstration, superhydrophobicity and anisotropic wetting behavior are revealed.

Introduction.

A hierarchy can be described as a structure in which different elements are placed according to levels of importance, being the structural elements structured themselves. The hierarchical order "n" can be described as the number of levels with recognized structure.[1] Multilevel structural organizations are recurrently observed in nature bestowing biological materials with exceptional properties.[2-4] As such, the hierarchical structures found in nature have been a source of inspiration for the development of multifunctional materials.[5] Superhydrophobic hierarchical nano and micro structures have been fabricated inspired on the fine hierarchical topography observed on the lotus leaf.[6-8] Dry-adhesive surfaces have been fabricated based on the branched nanopillars observed in the gecko feet.[9-10] The iridescence of the butterfly wings or the wettability of the rose petal have been reproduced as well by mimicking their stratified topologies.[11-12] The properties arising in each case relay on the existence of a fine hierarchical organization of features with sizes from the nanoscale to the microscale. The practical value of engineered hierarchical topographies has been recognized in different fields of application such as energy harvesting,[13] membrane technology,[14] anti-icing or anti-corrosion coatings,[15] photonics,[16] tissue

engineering,[17] micro/nano fluidics[18] among others. Engineering hierarchical micro-nano topographies is not a trivial task and as such, it is easy to understand that many efforts have been devoted to the development of suitable fabrication protocols to produce functional surfaces based on multilevel topographies in a practical and reproducible manner.

The simplest bottom-up approach to produce hierarchical architectures particularly effective to impart superhydrophobic self-cleaning properties includes surface coatings with particles of different sizes.[8, 19-20] Roughening of surfaces containing pre-patterned micron-sized structures has been also a straightforward approach employed. The roughening step include processes such as plasma treatment of polymeric topographies,[19, 21] physicochemical etching[22-23] or nanoparticle coating onto a micro-topography to confer a secondary rough pattern.[24] Additional approaches to produce double scale textures have taken advantage of wrinkling or swelling process.[25-26] The main limitation of these approaches is the lack of control of the topography at the nanometric level, resulting in a randomly distributed and often irregular secondary structure. While these topographies can be useful as superhydrophobic self-cleaning surfaces, they may have limited application in other areas.

Top-down approaches involving lithographic processes typically confer a higher degree of control over the generated structures. Combinations of several of these techniques have allowed fabricating hierarchical topographies with well-defined geometries. For instance, the combination of nanoimprint (NIL) and photolithographic processes to produce hierarchical structures was first described by X. Cheng and J. Guo for the fabrication of multiscale patterns in one-step.[27] This process involves the use of hybrid mask-mold prepared on purpose including the nanoscale patterns and a metal mask layer. The

preparation of such hybrid mask-mold entails however, a complex fabrication process of several steps.[28]

Capillary force nanoimprinting has been combined with UV-lithography and deep UV flood exposure by the group of H.C. Scheer to produce a series of 3D and multi-level structures.[29] Two-scale hierarchical structures combining different micro and nanoscale structures have been demonstrated by two-step temperature-directed capillary molding process[30] or two-step UV-assisted capillary force lithography.[31] However, these processes require strict control of the processing parameters, particularly related to the interfacial forces and viscosity of the polymeric material. C. Zhang and coworkers made use of the thermoplastic properties of the commercial epoxy based photoresist SU-8, and its photosensitive character to fabricate through CFL in combination with photopatterning, hierarchical pillar array structures with variable aspect ratio.[32] Electrohydrodynamic structures generated through polymer film instabilities by electrostatic pressure have also been produced onto thermal nanoimprinted structures to create dual-scale hierarchical topographies.[33]

In all the cases described above, like in the vast majority of hierarchical structures produced, the final topography consists of micron sized features with nanofeatures placed on top of these. Thus, the second-scale nanostructure is limited to the top surface of the micro-scale topography. As will be shown later, the process described in this paper overcomes this limitation by allowing to produce tailored nanopatterns covering the top and bottom regions of microstructured surfaces.

In more recent works, by combining Thermal NIL (T-NIL) and UV-NIL, Steinberg *et al.*[34-35] demonstrated the fabrication of more complex 3D hierarchical structures where the nanostructures covered the entire micron-scale topography. The procedure involved nanopatterning of a SU-8 precursor film by conventional T-NIL and, after partial surface hardening by a vacuum ultraviolet (VUV) treatment where the surface-near only is exposed to fix the nanostructures at the surface, a second T-NIL is performed using a mold containing the micrometric motifs to produce the micron level hierarchy. While this fabrication process allows for the entire surface to be covered with nanostructures, it still presents some limitations such as the narrow processing window for the VUV treatment, the need of a sacrificial mold and the compromise between the quality of the nanostructure and the aspect ratio of the microstructure. Another approach for the fabrication of hierarchical patterns with nanopatterns distributed at two different levels was developed in PDMS by Chen *et al.*[36] In this case, a microstructure is produced after the nanotopography in a second step of ultratraviolet-ozone exposure through a micron-size grid which leads to conversion and densification of the PDMS within the exposed areas resulting on the micron relief features. Although a simple approach, the feature depth achieved is limited to about 1 μm and the nanotopography is bound to be the same at the top and bottom of the microtopography.

Fabrication processes to produce multilevel hierarchical topographies are scarce in literature. Only recently, Cho and co-workers have presented a remarkable demonstration of multilevel multiscale micro-nano architectures.[37] The authors developed what they call multiplex lithography where the strategy in the process is the control of the spatial penetration of oxygen at the surface of a UV curable resin layer to render a polymer film

that can be further surface imprinted or bounded selectively at the different surfaces. Thus, it allows for a LEGO-like stacking of micrometre membranes layers together with the formation of multiscale patterns. Nonetheless, the process demands a high level of control during the multiple curing steps and it is restricted to UV-crosslinkable materials.

This work presents an easy-to-implement fabrication process that allows for the fabrication of multilevel hierarchical structures where the micro and nano-size geometrical features can be designed independently at different levels with very high feature control. The process can be applied over large areas providing a versatile approach to fabricate a large variety of multilevel multiscale hierarchical topographical designs that can be translated to any suitable polymeric material via NIL.

The versatility of the process allows for broad applicability in several fields. To demonstrate a practical usage of the multiscale hierarchical structures, superhydrophobicity and directional wetting are successfully demonstrated.

Results and Discussion

The fabrication process to produce multilevel hierarchical structures comprises three steps as schematically depicted in Figure 1 (top row). It involves initially performing NIL on a first layer of polymeric material to create the first nanopatterned layer. In a second step, a photoresist layer is spin coated on top of this layer and patterned by a second NIL process. The approach relays on the fact that conventional photo-resins show in fact a thermoplastic behavior.[29, 38] Lastly, photolithography of micron features is performed by maskless direct laser writing. After developing the photoresist, a hierarchical topography is

revealed. The process allows for different customization of nanopatterns on the two different levels with high fidelity.

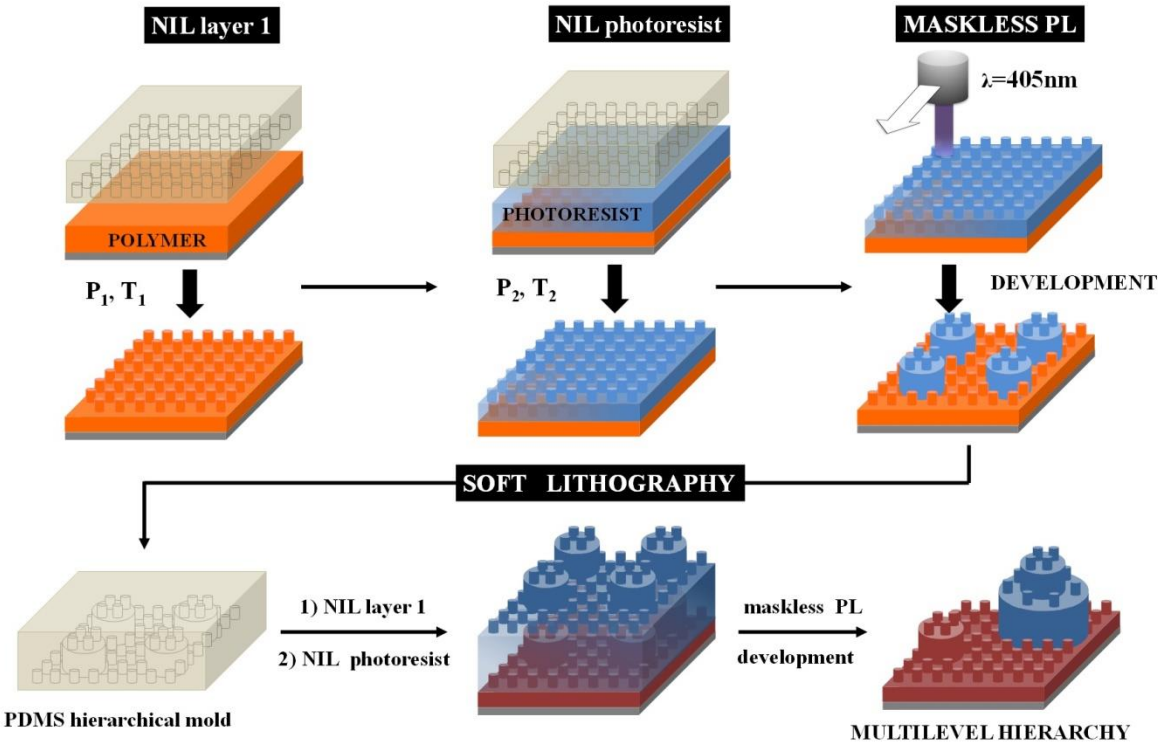

Figure 1. Outline of the fabrication process to produce multilevel and 3D fractal-like hierarchical structures. First, a layer of PMMA is spin coated on a Si wafer and imprinted with a nanotopography. Second, a photoresist layer is spin coated on it and imprinted with the same o different nanofeatures. Third, photolithography of micron size features is performed by direct laser writing. After development of the exposed resist, it is eliminated and the hierarchical topography containing nanostructures at different levels is revealed. A hierarchical mold can be obtained from replication by soft-lithography from the two-level topography. It can be then employed to perform subsequent replications increasing the hierarchical order.

The first layer can be a thermoplastic, a thermosetting or a UV cross-linkable polymer. For the second layer, a positive photoresist was employed throughout; however, other suitable photo-resins for the desired topographical design could be chosen. It is worth to note that the photolithographic step could also be performed by light exposure through a traditional photomask containing the features to pattern (an example of this process showing a two-level, third-order, hierarchical structure can be seen in Figure S1).

Figure 2 shows different hierarchical topographies produced by the process described illustrating the structure versatility and accuracy of the process. The hierarchical topographies include a first layer of polymethylmethacrylate (PMMA) thin film (300 nm) deposited by spin coating and a second layer of a photo-resin (AZ 1512, 2 μm in thickness) spin coated over the previously imprinted layer. For the NIL process, a PDMS replica molds with different nanoscopic scale features were employed (500 nm period nano gratings and anti-reflective moth-eye like nanocone hexagonal array). Several hierarchical patterns were produced by different combinations of these two molds for the top or the bottom imprinting steps with different microstructures (pillars, grooves, cubes, etc)

When using thermoplastic polymers, it is necessary to select among those with sufficiently high glass transition temperature (T_g) to avoid softening of the material and keeping the structural integrity of the first imprinted layer during the second step of thermal NIL onto the photo-resin. To avoid this potential issue, alternatively a UV-crosslinked thermosetting resin for the first layer can be employed such that the second thermal imprint process should not cause deformation of the nanostructures. The layer combination of UV-curing and thermosetting resins will allow for a large degree of flexibility during the consecutive processing steps.

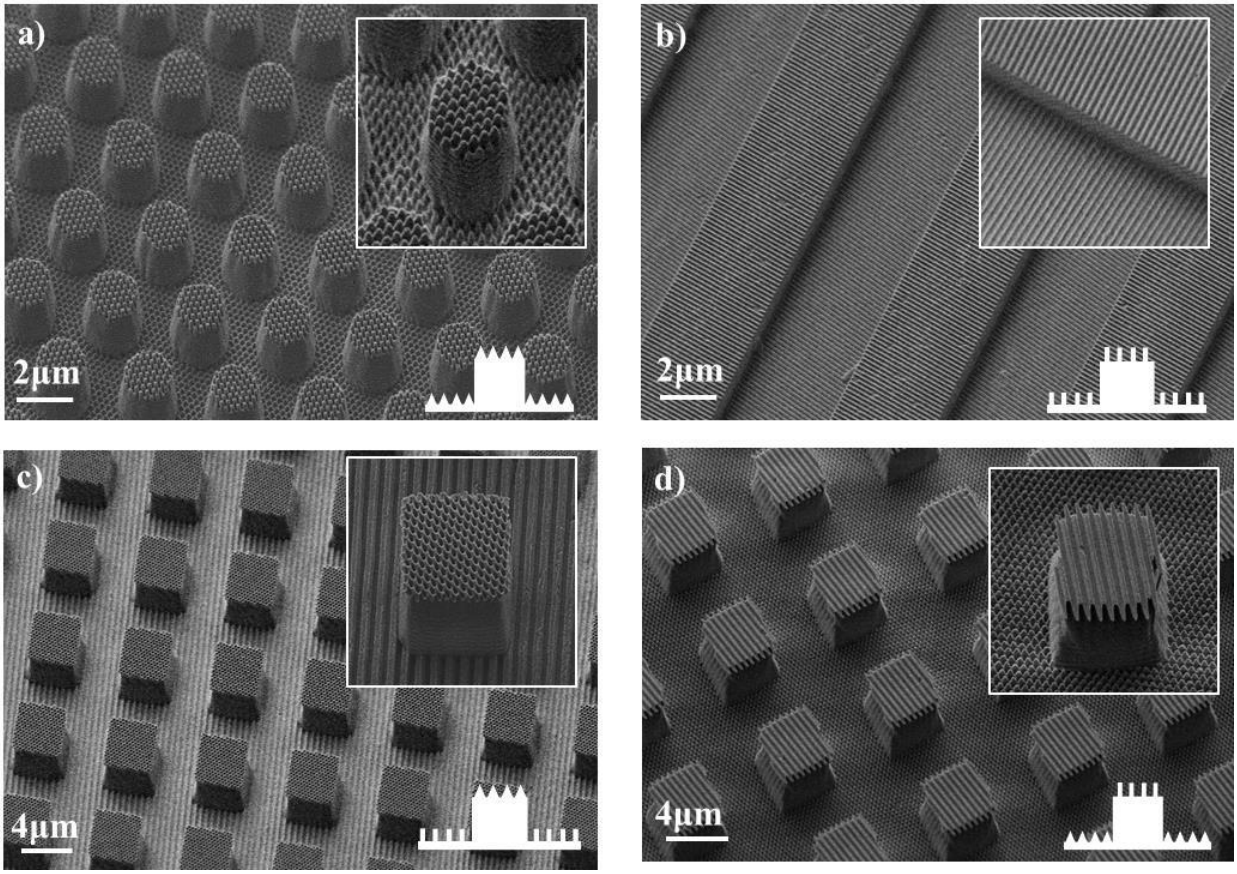

Figure 2. SEM images of two-level, third order, hierarchical structures showing combinations of moth-eye topography or 500 nm period gratings at two different levels of micron-size features (pillars, grooves or cubes) obtained by maskless photolithography. The insets show expanded view of the nanofeatures and schematics of the corresponding hierarchical structures produced in each case.

Figure 3 shows a two-level, third order, hierarchical structure generated using an epoxy resin (Epo-Tek) for the first patterned layer and a photo-resin for the second one as done previously. Three different structures can be identified on it: a bottom layer consisting on a square array of nano-pillars (500 nm in diameter, 2 µm in height) produced by UV-NIL on

the epoxy resin, a second hexagonal array of micro-pillars (20 μm in diameter, 4 μm in height) fabricated by direct laser writing on the photo resin and located on the top surface of these microstructures, a third level comprising a moth-eye like nanocones produced by the second T-NIL step prior to the laser writing step. In the image, parallel contrast lines are perceived on top of the micropillars which correspond to Moirè fringes caused by the mismatch in pitch between the moth-eye topography and the electron beam raster scan. These are produced only at that the low magnification while at higher magnification (image inset), Moirè patterns are not formed.[39]

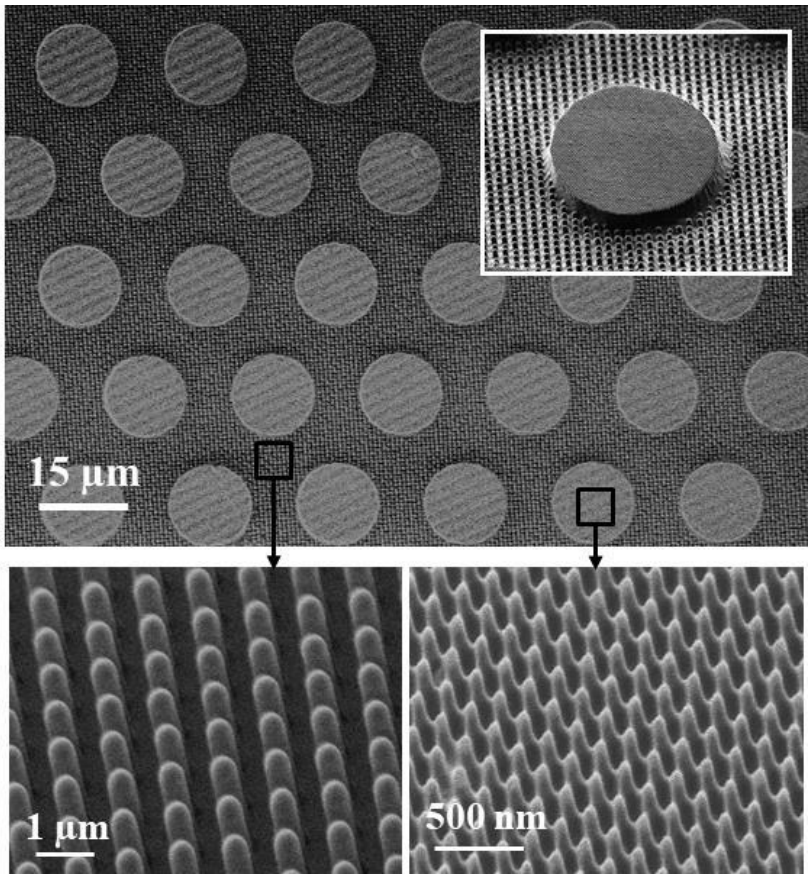

Figure 3. SEM images of a two-level, third order hierarchical structure including 0.5x2 μm rectangular pillar array and 20x4 μm pillar hexagonal array on the first level and a moth-eye nanocone hexagonal topography on the second.

The complexity of the hierarchical topography was further increased in a practical and reproducible manner to produce multilevel-hierarchical structures in a 3D fractal-like structural arrangement. The process is outlined in Figure 1 (bottom row). It begins by making a PDMS replica mold of the two-level hierarchical structures already produced. The two-level hierarchical molds are then employed during the imprinting steps of the first polymer layer and photo-resin. Laser maskless lithography is finally carried out to produce the micron size features, obtaining upon development, a multilevel-hierarchical topography with extremely high accuracy. It should be remarked that the hierarchical topographies are initially produced in two different materials. By soft lithography, a replica mold is produced and employed for the NIL process to produce hierarchical structures into any desired polymer, being the final substrate a homogeneous material (Figure S2).

The sole requirement to produce this multilevel hierarchy is that the size of the features during this second lithographic process should have an area bigger than that of previous step to accommodate several features. Remarkably, the enclosed features are thus self-aligned into the previous level and, therefore, tedious alignment processes for many of the designs can be obviated. Should the structural design require alignment, it could be nevertheless performed through alignment marks.

By repeating the process sequentially, a linear growth of the hierarchical order and scale levels can be achieved, generating 3D fractal-like structures with increasing complexity.

The limit on the number of layers to possibly accommodate will vary depending on the geometrical dimensions of the different levels and will be given by the photolithographic step and the nanoimprinting and de-molding processes as the aspect ratio and complexity of the architectures increases.

An example of a third-order, four-level multi-scale topography produced by this process is shown in Figure 5. To produce this complex hierarchy, a first layer of a UV curing epoxy resin was casted and subsequently imprinted by UV-NIL. The mold employed here for the imprinting step was obtained by replication via soft-lithography from the two-level, third-order hierarchical structures obtained before (Figure 2a). Hence, after the first NIL step two-level hierarchical structures are produced on the bottom layer. Then, a second layer of photoresist was spin coated, in this case the AZ9260 photo-resin was employed because it allows for thicker films (up to 20 μm in a single coating step). This second layer was then imprinted with the same two-level, third order hierarchical mold and afterwards, the exposed photo-resin was developed. Figure 5 shows that the two-level hierarchical topography can be found on top and bottom of the larger micropillar array. As it can be observed, moth-eye nanostructures are located at four different levels.

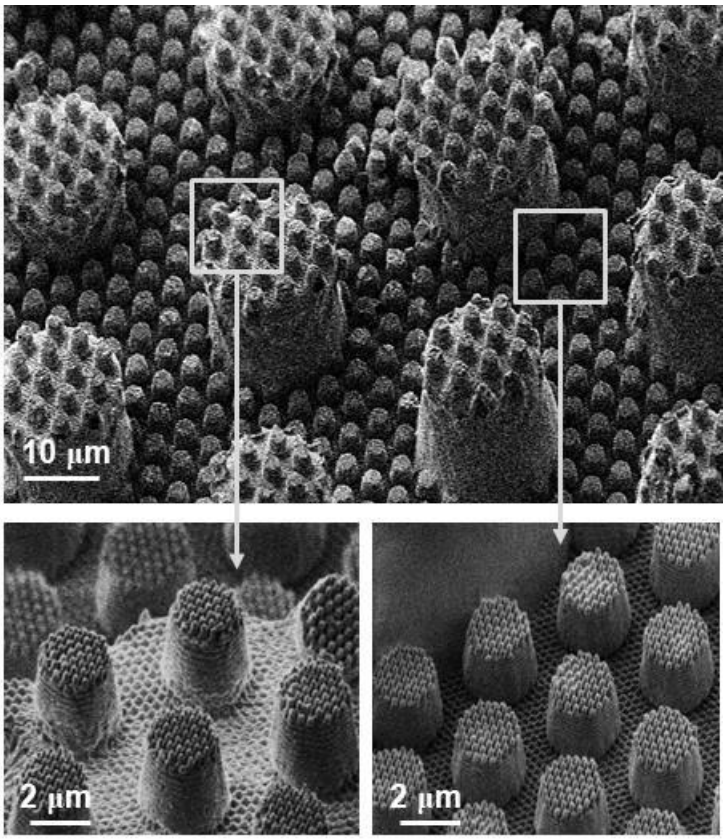

Figure 5. SEM images of 3D fractal-like multilevel hierarchical structures. A moth-eye topography can be found on four different levels coexisting with micropillars arrays of two different dimensions (2x2 and 15x20µm).

The versatility of the process can be applied to create hierarchical surfaces with controlled wetting properties such as superhydrophobicity or anisotropic wetting.

The wetting behavior of several patterned surfaces was characterized by static water contact angle (WCA) measurements (Figure S4). Then, the wetting characteristics of the hierarchical textures were compared with those of the corresponding simple nano and micro patterns. For this experiment, the microscale topography employed consisted of 2 µm micropillar array with low aspect ratio (AR=1), the nanoscale topography comprised moth-

eye-like nanocone features and the hierarchical topography combining both, the 2x2 μm micropillars and moth-eye nanotextures at the two-levels of the micropillars (SEM images of the hierarchical surfaces are shown in Figure S3). The topography was produced in several materials since it is known that the wetting properties of a surface depend on its composition and related surface energy as well as on the surface topography. Figure 6 compares the static WCA values obtained on the various materials. In all cases, it was observed an increase of the WCA upon surface texturization, with a more pronounced increment seen on the moth-eye nanotextures. In fact, for the hydrophobic, PFPE and PDMS materials tested, upon nanopatterning, the surfaces become superhydrophobic reaching WCA above 150º. In the less hydrophobic PMMA, superhydrophobicity only arises upon patterning with hierarchical features. The role for both length scale structures on the surface mimicking the lotus topography has been widely documented before. [6-7, 40]

Another useful surface behavior is directional wetting. Surfaces showing unidirectional liquid flow due to anisotropic wetting can find applications in many different fields such as microfluidics systems or in many ink printing technologies.[41-43] To test this property, several hierarchical structures comprising microgrooves (6 μm width, 12 μm period and 2 μm height) and nano gratings (500 nm period) oriented parallel or perpendicular to the microgrooves, or with moth-eye nanocone structures were fabricated and the wetting behavior characterized and compared to that of simple micro grooves.

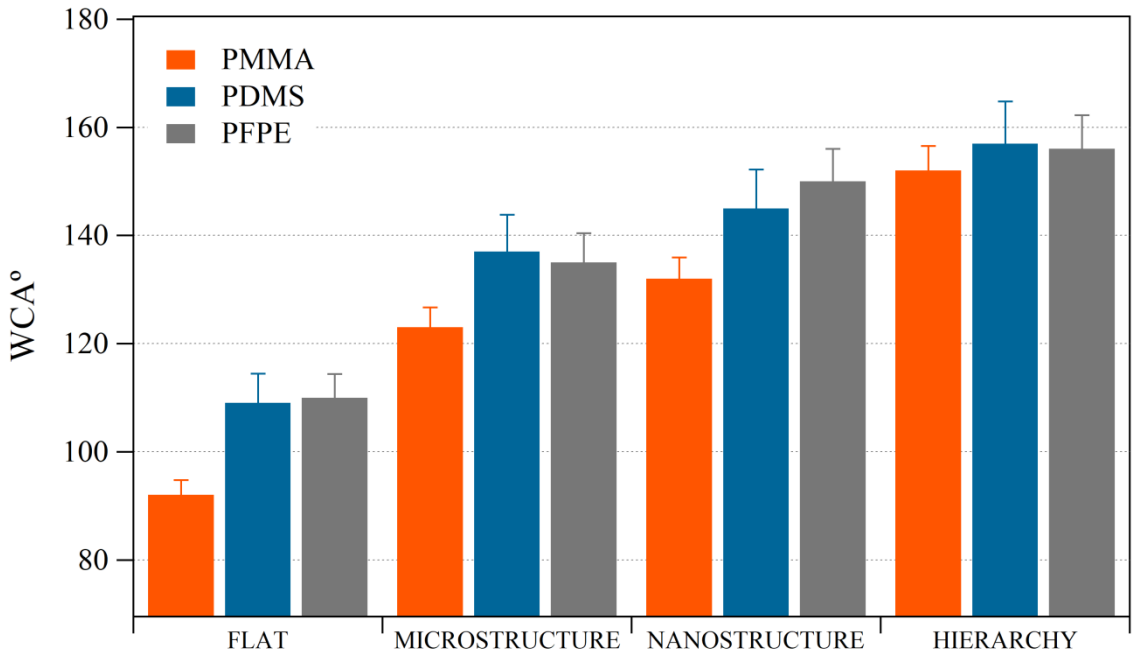

Figure 6. Static water contact angle measurements obtained on a second-order two-level hierarchical topography of 2x2 µm micropillars and moth-eye nanocones made on three different materials as noted on the chart comparatively to the flat surface of the corresponding material, and the simple micro and nano topographical components of the hierarchy.

The patterns were created on a 2 µm thick AZ1512 resist film. The investigation of the directional wetting properties of these surfaces was carried out by WCA measurements. The WCA measured on a flat resist film showed values of about 100±4º (Figure S5). Figure 7 shows images of the water droplets deposited on the substrates with different nano/micro patterns taken parallel or perpendicular to the micro microgroove direction. The images shown were taken 10 seconds after drop deposition and the corresponding WCA values are indicated in each case. It can be seen that all the surfaces exhibited a certain degree of

anisotropic wetting caused by the geometrical anisotropy of the microgrooves. However, directional wetting where the water droplet spreads in the direction parallel to the hierarchical microgrooves was only seen on the hierarchical topography with the nano grating direction placed parallel to that of the microgroove This can be observed in Figure 7b given by the dramatic reduction in the value of WCA in the parallel direction (Video S1 shows the drop dynamic spreading). The mobility of the water in this direction was indeed enhanced such that the droplet can be drag along the surface using a dispensing needle (Video S2). Conversely, the hierarchical surfaces where the nanostructures at the second level involve nano gratings placed perpendicular to the microgrooves or moth-eye nanocones do not show a significant directional wetting.

Directional wetting in grating structures has been observed before and it has been ascribed to the larger energy barrier water droplets experience as they try to spread along the direction perpendicular to the grooves. [44-46] Hence, the results presented here underscore the need for patterns with geometrical anisotropy to achieve directional wettability.

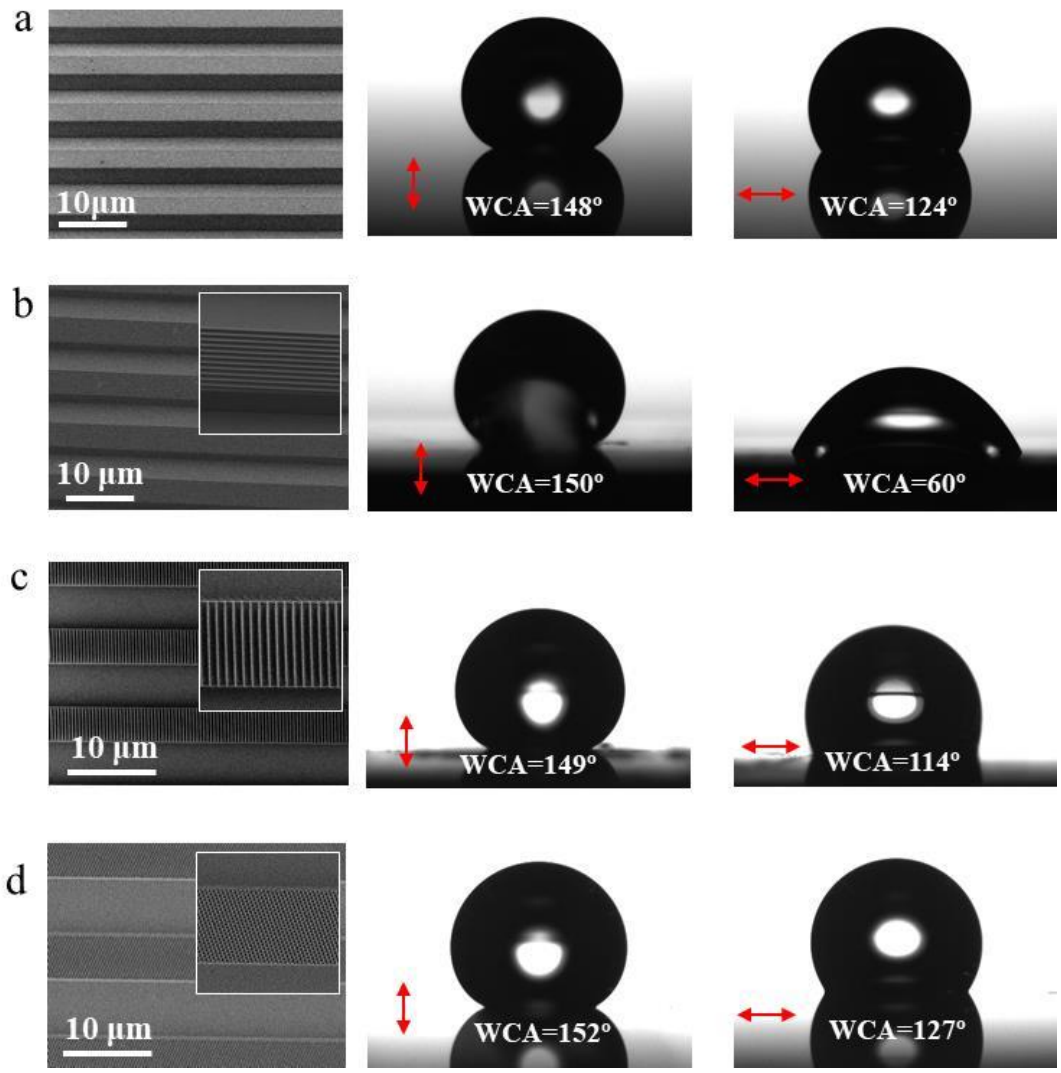

Figure 7. SEM images of hierarchical surfaces and pictures of drops deposited in each of them taken 10 seconds after dispensing for a microstructured surface (a), a hierarchical surface with nano gratings parallel to the microgroove direction (b), a hierarchical surface with nano gratings perpendicular to the microgrove (c) and a hierarchical surface with moth-eye nanocone structures on top of microgrooves (d). The images were taken in the direction parallel and perpendicular to the microgroove direction as indicated by the red arrow.

Conclusions

Complex multilevel hierarchical structures have been generated in a practical and reproducible manner by an approach combining consecutive nanoimprintings with a photolithographic process. The methodology developed allows defining precisely the specific nano and microstructure geometry implicated at each level. Furthermore, using this methodology, self-similar 3D structures at reducing length-scales can also be produced in a sort of fractal fashion.

Multilevel hierarchical structures that combine nano and microscale features generate complex physical environments that allow for new properties and for testing surface interactions of different length scales at once. As illustration of the relevance of the methodology, exemplary superhydrophobic surfaces and surfaces with controlled anisotropic wetting have been demonstrated.

This work represents an easy-to-implement fabrication process for future development of multilevel hierarchical structures with very high feature control over large areas.

Experimental Methods

Different polymers were employed for the preparation of the different hierarchical surfaces including the thermoplastic polymethylmethacrylate (950-PMMA, Microchem), UV curable epoxy resin (Epo-Tek OG142), the thin positive photoresist (AZ1512, MicroChem) and the thick positive photoresist (AZ9260, MicroChem). The desired layer thickness in each case was controlled by adjusting the spin coating conditions.

The nanometer size feature molds were replicated by soft lithography using hard polydimethylsiloxane (h-PDMS).[47] Working molds of PDMS with the moth-eye topography and 500 nm period microridges were prepared by replicating a master nickel (HT-AR-02, Temicon) and a silicon (LightSmyth Technologies) molds respectively using the procedure described elsewhere.[48]

For the fabrication of the hierarchical multilevel structures, the first step was the production of the two-level second order hierarchical h-PDMS working mold. The substrates obtained on the sequential replication steps are illustrated by SEM images in Figure S2. In this example, a two-level hierarchical structure containing moth-eye like nanocones on top and bottom of a micron size pore array, created by maskless lithography, was first replicated by an acrylic perfluoropolyether (PFPE)(MD700 Fluorink) [49-50] by UV photocrosslinking using 2.5% w/w initiator (2-hydroxy-2-methylpropiophenone, Aldrich) and a UV light providing *ca*. 80 $mW \cdot cm^{-2}$ (UVASPOT 400/T Honle). Subsequently, the hierarchical topography was replicated into a h-HDMS working mold using a similar procedure to that described previously.[38]

The UV-NIL and T-NIL processes were accomplished by using an EITRE3 Nano Imprint Lithography system (Obducat). The imprinting parameters were adjusted in each case to the requirements of the material; Table 1 summarizes the conditions employed:

Table 1. T-NIL and UV-NIL conditions

Material	**T (ºC)**	**P (bar)**	**t (s)**	**UV light**
PMMA	170	30	300	NO
EpoTek	60	15	180	YES
AZ1512	100	30	180	NO
AZ9260	100	30	180	NO

T = temperature, P= pressure, t=time

Optical lithography was performed using a maskless laser writer (Heidelberg DWL66) equipped with a 405 nm diode laser to pattern the AZ resists. A 4 mm focal length writing head was used, which typically yields features size down to 800 nm.

The AZ1512 resist was spin coated at 2000 rpm to obtain films with 2 μm in thickness and baked for 1 min at 90 ºC. The AZ9260 was spin coated at 2000 rpm to yield 15 um thick films, and baked at 110 ºC for 2 min.

The photoresist development processes were carried out by using the standard AZ 351B (for AZ1512 resist) and AZ 400 (for AZ 9260, diluted on DI water to a 1:4 ratio) developers. The development time needed varied from 1 min for AZ1512 to 4 min for AZ9260.

The static water contact angle measurements were performed using an optical tensiometer (Attension Theta, Biolin Scientific). For this, deionized water droplets of 4 μL were gently deposited onto the substrate to prevent the drops from rolling off. Figure S4 shows images of the drops deposited over the different films surfaces with the corresponding WCA.

The topography of the multilevel hierarchical structures was characterized by using a scanning electron microscopy (SEM) (FSEM Auriga, Carl Zeiss) working on a low voltage (1KV) and current (10 pA) mode to avoid damaging the nanostructures. It was found out that the appearance of the moth-eye topography is strongly directional and only at the right imaging angle, the nanocones full height can be appreciated. Hence, this effect has to be considered for proper imaging of the nanocone structures (see Figure S6).

ASSOCIATED CONTENT

Supporting Information is available free of charge on the ACS Publications website: Description of the replication procedure; SEM characterization of textured surfaces; wetting characterization; angular dependence of moth-eye topography characterized by SEM (Figures S1-S6 and Videos S1-S2).

AUTHOR INFORMATION

Corresponding Author

*Jaime J. Hernández Rueda IMDEA Nanoscience.

c/ Faraday 9, Campus Universitario de Cantoblanco, 28049 Madrid, Spain.

Tel. +34 91 299 87 00

E-mail: jaime.hernandez@imdea.org

Author Contributions

The manuscript was written through contributions of all authors. All authors have given approval to the final version of the manuscript.

Funding Sources

This work was supported by the Spanish Ministerio de Industria, Economía, y Competitividad through project BiSURE (Ref no: DPI2017-90058-R) and the 'Severo Ochoa' Programme for Centres of Excellence in R&D (MINECO, Grant SEV-2016-0686). M.T.A. acknowledges a grant from the Ministry of Education and Research of the Madrid Community and European Social Fund (ESF) (ref. PEJD-2016/IND-2899).

ACKNOWLEDGMENT

The authors gratefully acknowledge to Mrs. Alejandra Jacobo for her valuable assistance regarding mold replication and imprinting of the moth-eye structures. The authors also thank Dr. Daniel Granados for his support at the IMDEA Nanofabrication Center.

References

1. Lakes, R., Materials with structural hierarchy. *Nature* **1993,** *361*, 511.
2. Won-Gyu, B.; Nam, K. H.; Doogon, K.; Suk-Hee, P.; Eui, J. H.; Kahp-Yang, S., 25th Anniversary Article: Scalable Multiscale Patterned Structures Inspired by Nature: the Role of Hierarchy. *Advanced Materials* **2014,** *26* (5), 675-700.
3. Brodoceanu, D.; Bauer, C. T.; Kroner, E.; Arzt, E.; Kraus, T., Hierarchical bioinspired adhesive surfaces—a review. *Bioinspiration & Biomimetics* **2016,** *11* (5), 051001.
4. Zhang, C.; McAdams, D. A.; Grunlan, J. C., Nano/Micro-Manufacturing of Bioinspired Materials: a Review of Methods to Mimic Natural Structures. *Advanced Materials* **2016,** *28* (30), 6292-6321.
5. Liu, K.; Jiang, L., Bio-inspired design of multiscale structures for function integration. *Nano Today* **2011,** *6* (2), 155-175.
6. Bhushan, B.; Jung, Y. C.; Koch, K., Micro-, nano- and hierarchical structures for superhydrophobicity, self-cleaning and low adhesion. *Philosophical Transactions of the Royal Society a-Mathematical Physical and Engineering Sciences* **2009,** *367* (1894), 1631-1672.
7. Ho, A. Y. Y.; Luong Van, E.; Lim, C. T.; Natarajan, S.; Elmouelhi, N.; Low, H. Y.; Vyakarnam, M.; Cooper, K.; Rodriguez, I., Lotus bioinspired superhydrophobic, self-cleaning surfaces from hierarchically assembled templates. *Journal of Polymer Science Part B: Polymer Physics* **2014,** *52* (8), 603-609.
8. Lu, Y.; Sathasivam, S.; Song, J.; Crick, C. R.; Carmalt, C. J.; Parkin, I. P., Robust self-cleaning surfaces that function when exposed to either air or oil. *Science* **2015,** *347* (6226), 1132-1135.
9. Raut, H. K.; Baji, A.; Hariri, H. H.; Parveen, H.; Soh, G. S.; Low, H. Y.; Wood, K. L., Gecko-Inspired Dry Adhesive Based on Micro–Nanoscale Hierarchical Arrays for Application in Climbing Devices. *ACS Applied Materials & Interfaces* **2018,** *10* (1), 1288-1296.
10. Ho, A. Y. Y.; Yeo, L. P.; Lam, Y. C.; Rodríguez, I., Fabrication and Analysis of Gecko-Inspired Hierarchical Polymer Nanosetae. *ACS Nano* **2011,** *5* (3), 1897-1906.
11. Feng, L.; Zhang, Y.; Xi, J.; Zhu, Y.; Wang, N.; Xia, F.; Jiang, L., Petal Effect: A Superhydrophobic State with High Adhesive Force. *Langmuir* **2008,** *24* (8), 4114-4119.
12. Zhang, S.; Chen, Y., Nanofabrication and coloration study of artificial Morpho butterfly wings with aligned lamellae layers. *Scientific Reports* **2015,** *5*, 16637.
13. Lu, X.; Li, T.; Bertei, A.; Cho, J. I. S.; Heenan, T. M. M.; Rabuni, M. F.; Li, K.; Brett, D. J. L.; Shearing, P. R., The application of hierarchical structures in energy devices:

new insights into the design of solid oxide fuel cells with enhanced mass transport. *Energy & Environmental Science* **2018**.
14. Cho, H.; Kim, J.; Park, H.; Won Bang, J.; Seop Hyun, M.; Bae, Y.; Ha, L.; Yoon Kim, D.; Min Kang, S.; Jung Park, T.; Seo, S.; Choi, M.; Suh, K.-Y., Replication of flexible polymer membranes with geometry-controllable nano-apertures via a hierarchical mould-based dewetting. *Nature Communications* **2014,** *5*, 3137.
15. Darmanin, T.; Guittard, F., Recent advances in the potential applications of bioinspired superhydrophobic materials. *Journal of Materials Chemistry A* **2014,** *2* (39), 16319-16359.
16. Wang, W.; Xu, J., Structure and Visible Light Luminescence of 3D Flower-like Co3O4 Hierarchical Microstructures Assembled by Hexagonal Porous Nanoplates. *ACS Applied Materials & Interfaces* **2015,** *7* (1), 415-421.
17. Domingues, R. M. A.; Gonçalves, A. I.; Costa-Almeida, R.; Rodrigues, M. T.; Reis, R. L.; Gomes, M. E., Chapter 10 - Fabrication of Hierarchical and Biomimetic Fibrous Structures to Support the Regeneration of Tendon Tissues. In *Tendon Regeneration*, Gomes, M. E.; Reis, R. L.; Rodrigues, M. T., Eds. Academic Press: Boston, **2015**, pp 259-280.
18. Feng, Y.; Zhu, W.; Guo, W.; Jiang, L., Bioinspired Energy Conversion in Nanofluidics: A Paradigm of Material Evolution. *Advanced Materials* **2017,** *29* (45), 1702773.
19. Ellinas, K.; Pujari, S. P.; Dragatogiannis, D. A.; Charitidis, C. A.; Tserepi, A.; Zuilhof, H.; Gogolides, E., Plasma Micro-Nanotextured, Scratch, Water and Hexadecane Resistant, Superhydrophobic, and Superamphiphobic Polymeric Surfaces with Perfluorinated Monolayers. *ACS Applied Materials & Interfaces* **2014,** *6* (9), 6510-6524.
20. Baidya, A.; Das, S. K.; Ras, R. H. A.; Pradeep, T., Fabrication of a Waterborne Durable Superhydrophobic Material Functioning in Air and under Oil. *Advanced Materials Interfaces* **2018,** *5* (11), 1701523.
21. Ferchichi, A. K.; Panabière, M.; Desplats, O.; Gourgon, C., Fabrication of superhydrophobic surfaces on flexible fluorinated foils by using dual-scale patterning. *Materials Research Express* **2014,** *1* (2), 025704.
22. Groten, J.; Rühe, J., Surfaces with Combined Microscale and Nanoscale Structures: A Route to Mechanically Stable Superhydrophobic Surfaces? *Langmuir* **2013,** *29* (11), 3765-3772.
23. Pozzato, A.; Zilio, S. D.; Fois, G.; Vendramin, D.; Mistura, G.; Belotti, M.; Chen, Y.; Natali, M., Superhydrophobic surfaces fabricated by nanoimprint lithography. *Microelectronic Engineering* **2006,** *83* (4–9), 884-888.
24. Kim, H.-K.; Cho, Y.-S., Fabrication of a superhydrophobic surface via spraying with polystyrene and multi-walled carbon nanotubes. *Colloids and Surfaces A: Physicochemical and Engineering Aspects* **2015,** *465* (0), 77-86.
25. Chen, C.-M.; Reed, J. C.; Yang, S., Guided wrinkling in swollen, pre-patterned photoresist thin films with a crosslinking gradient. *Soft Matter* **2013,** *9* (46), 11007-11013.
26. Rodríguez-Hernández, J.; del Campo, A., Fabrication of hierarchical wrinkled morphologies through sequential UVO treatments. *Journal of Applied Polymer Science* **2015,** *132* (17).
27. Cheng, X.; Jay Guo, L., One-step lithography for various size patterns with a hybrid mask-mold. *Microelectronic Engineering* **2004,** *71* (3), 288-293.

28. Schift, H.; Spreu, C.; Schleunitz, A.; Gobrecht, J.; Klukowska, A.; Reuther, F.; Gruetzner, G., Easy mask-mold fabrication for combined nanoimprint and photolithography. *Journal of Vacuum Science & Technology B: Microelectronics and Nanometer Structures Processing, Measurement, and Phenomena* **2009,** *27* (6), 2850-2853.
29. Dhima, K.; Steinberg, C.; Wang, S.; Papenheim, M.; Scheer, H.-C., Nanoimprint combination techniques. *Microelectronic Engineering* **2015,** *141*, 92-101.
30. Jeong, H. E.; Lee, S. H.; Kim, J. K.; Suh, K. Y., Nanoengineered Multiscale Hierarchical Structures with Tailored Wetting Properties. *Langmuir* **2006,** *22* (4), 1640-1645.
31. Ho, D.; Zou, J.; Zdyrko, B.; Iyer, K. S.; Luzinov, I., Capillary force lithography: the versatility of this facile approach in developing nanoscale applications. *Nanoscale* **2015,** *7* (2), 401-414.
32. Ying, Z.; Chia-Tai, L.; Shu, Y., Fabrication of Hierarchical Pillar Arrays from Thermoplastic and Photosensitive SU-8. *Small* **2010,** *6* (6), 768-775.
33. Tian, H.; Shao, J.; Hu, H.; Wang, L.; Ding, Y., Generation of Hierarchically Ordered Structures on a Polymer Film by Electrohydrodynamic Structure Formation. *ACS Applied Materials & Interfaces* **2016,** *8* (25), 16419-16427.
34. Steinberg, C.; Rumler, M.; Runkel, M.; Papenheim, M.; Wang, S.; Mayer, A.; Becker, M.; Rommel, M.; Scheer, H.-C., Complex 3D structures via double imprint of hybrid structures and sacrificial mould techniques. *Microelectronic Engineering* **2017,** *176*, 22-27.
35. Steinberg, C.; Papenheim, M.; Wang, S.; Scheer, H.-C., Complex 3D structures via hybrid processing of SU-8. *Microelectronic Engineering* **2016,** *155*, 14-18.
36. Chen, Y.; Wang, Z.; Kulkarni, M. M.; Wang, X.; Al-Enizi, A. M.; Elzatahry, A. A.; Douglas, J. F.; Dobrynin, A. V.; Karim, A., Hierarchically Patterned Elastomeric and Thermoplastic Polymer Films through Nanoimprinting and Ultraviolet Light Exposure. *ACS Omega* **2018,** *3* (11), 15426-15434.
37. Cho, H.; Moon Kim, S.; Sik Kang, Y.; Kim, J.; Jang, S.; Kim, M.; Park, H.; Won Bang, J.; Seo, S.; Suh, K.-Y.; Sung, Y.-E.; Choi, M., Multiplex lithography for multilevel multiscale architectures and its application to polymer electrolyte membrane fuel cell. *Nature Communications* **2015,** *6*, 8484.
38. Dhima, K.; Steinberg, C.; Möllenbeck, S.; Mayer, A.; Wang, S.; Sheer, H.-C., Experimental analysis for process control in hybrid lithography. *Journal of Vacuum Science & Technology B* **2011,** *29* (6), 06FC14.
39. Read, D. T.; Dally, J. W. In *Theory of Moiré Fringe Formation with an Electron Beam*, Dordrecht, Springer Netherlands: Dordrecht, **2002**; pp 99-108.
40. Koishi, T.; Yasuoka, K.; Fujikawa, S.; Ebisuzaki, T.; Zeng, X. C., Coexistence and transition between Cassie and Wenzel state on pillared hydrophobic surface. *Proceedings of the National Academy of Sciences* **2009,** *106* (21), 8435-8440.
41. Xu, C.; Feng, R.; Song, F.; Wu, J.-M.; Luo, Y.-Q.; Wang, X.-L.; Wang, Y.-Z., Continuous and controlled directional water transportation on a hydrophobic/superhydrophobic patterned surface. *Chemical Engineering Journal* **2018,** *352*, 722-729.
42. Kooij, E. S.; Jansen, H. P.; Bliznyuk, O.; Poelsema, B.; Zandvliet, H. J. W., Directional wetting on chemically patterned substrates. *Colloids and Surfaces A: Physicochemical and Engineering Aspects* **2012,** *413*, 328-333.

43. Si, Y.; Wang, T.; Li, C.; Yu, C.; Li, N.; Gao, C.; Dong, Z.; Jiang, L., Liquids Unidirectional Transport on Dual-Scale Arrays. *ACS Nano* **2018,** *12* (9), 9214-9222.
44. Zhang, F.; Low, H. Y., Anisotropic Wettability on Imprinted Hierarchical Structures. *Langmuir* **2007,** *23* (14), 7793-7798.
45. Xia, D.; He, X.; Jiang, Y.-B.; Lopez, G. P.; Brueck, S. R. J., Tailoring Anisotropic Wetting Properties on Submicrometer-Scale Periodic Grooved Surfaces. *Langmuir* **2010,** *26* (4), 2700-2706.
46. Tawfick, S.; De Volder, M.; Copic, D.; Park, S. J.; Oliver, C. R.; Polsen, E. S.; Roberts, M. J.; Hart, A. J., Engineering of Micro- and Nanostructured Surfaces with Anisotropic Geometries and Properties. *Advanced Materials* **2012,** *24* (13), 1628-1674.
47. Schmid, H.; Michel, B., Siloxane Polymers for High-Resolution, High-Accuracy Soft Lithography. *Macromolecules* **2000,** *33* (8), 3042-3049.
48. Navarro-Baena, I.; Jacobo-Martín, A.; Hernández, J. J.; Castro Smirnov, J. R.; Viela, F.; Monclús, M. A.; Osorio, M. R.; Molina-Aldareguia, J. M.; Rodríguez, I., Single-imprint moth-eye anti-reflective and self-cleaning film with enhanced resistance. *Nanoscale* **2018**, 15496-15504.
49. Williams, S. S.; Retterer, S.; Lopez, R.; Ruiz, R.; Samulski, E. T.; DeSimone, J. M., High-Resolution PFPE-based Molding Techniques for Nanofabrication of High-Pattern Density, Sub-20 nm Features: A Fundamental Materials Approach. *Nano Letters* **2010,** *10* (4), 1421-1428.
50. Bong, K. W.; Lee, J.; Doyle, P. S., Stop flow lithography in perfluoropolyether (PFPE) microfluidic channels. *Lab on a Chip* **2014,** *14* (24), 4680-4687.

For Table of Contents Only